

OAK RIDGE
NATIONAL LABORATORY

MANAGED BY UT-BATTELLE
FOR THE DEPARTMENT OF ENERGY



ORNL-27 (4-00)

DOCUMENT AVAILABILITY

Reports produced after January 1, 1996, are generally available free via the U.S. Department of Energy (DOE) Information Bridge.

Web site <http://www.osti.gov/bridge>

Reports produced before January 1, 1996, may be purchased by members of the public from the following source.

National Technical Information Service
5285 Port Royal Road
Springfield, VA 22161
Telephone 703-605-6000 (1-800-553-6847)
TDD 703-487-4639
Fax 703-605-6900
E-mail info@ntis.fedworld.gov
Web site <http://www.ntis.gov/support/ordernowabout.htm>

Reports are available to DOE employees, DOE contractors, Energy Technology Data Exchange (ETDE) representatives, and International Nuclear Information System (INIS) representatives from the following source.

Office of Scientific and Technical Information
P.O. Box 62
Oak Ridge, TN 37831
Telephone 865-576-8401
Fax 865-576-5728
E-mail reports@adonis.osti.gov
Web site <http://www.osti.gov/contact.html>

This report was prepared as an account of work sponsored by an agency of the United States Government. Neither the United States Government nor any agency thereof, nor any of their employees, makes any warranty, express or implied, or assumes any legal liability or responsibility for the accuracy, completeness, or usefulness of any information, apparatus, product, or process disclosed, or represents that its use would not infringe privately owned rights. Reference herein to any specific commercial product, process, or service by trade name, trademark, manufacturer, or otherwise, does not necessarily constitute or imply its endorsement, recommendation, or favoring by the United States Government or any agency thereof. The views and opinions of authors expressed herein do not necessarily state or reflect those of the United States Government or any agency thereof.

Results from ORNL Characterization of Nominal 350 μm LEUCO Kernels (LEU03) from the BWXT G73V-20-69303 Composite

A. K. Kercher and J.D. Hunn, Oak Ridge National Laboratory

This document is a compilation of characterization data obtained on the nominal 350 μm diameter low enrichment uranium oxide/uranium carbide kernels (LEUCO) from the BWXT G73V-20-69303 composite. This kernel composite has been designated as LEU03 by Oak Ridge National Laboratory. It was produced by BWXT for the Advanced Gas Reactor Fuel Development and Qualification Program (AGR) for use in fabricating fuel for irradiation tests AGR-3 and AGR-4. LEU03 is a 510 g composite of two batches produced at BWXT and shipped to ORNL in July 2006. Before characterization or use at ORNL, LEU03 kernels were hand-tabled to remove 0.37 grams of debris and irregularly shaped particles. ORNL has performed size, shape, density, and microstructural analysis on riffled samples from the kernel composite.

Table of Contents

1	<i>Summary of results</i>	5
2	<i>Size and shape measurement (Kercher, Hunn, Price)</i>	7
2.1	<i>Description of method</i>	7
2.2	<i>Size and aspect ratios</i>	7
3	<i>Optical and electron microscopy of kernel surfaces (Hunn, Menchhofer, Kercher)</i>	10
3.1	<i>Type A kernels (shiny & smooth)</i>	11
3.2	<i>Type B kernels (dull & smooth)</i>	12
4	<i>Microscopy of kernel polished cross-sections (Hunn, Menchhofer, Kercher, Dunbar)</i>	13
5	<i>Density measurement (Hunn, Nunn)</i>	17
	<i>References</i>	18

1 Summary of results

Measurements were made using optical microscopy to determine the size and shape of the LEU03 kernels. Hg porosimetry was performed to measure density. The results are summarized in Table 1-1. Values in the table are for the composite and are calculated at 95% confidence from the measured values of a random riffled sample. The LEU03 kernel composite met all the specifications in Table 1-1.

Table 1-1. Summary of ORNL reported values of LEU03 versus kernel specification.

Kernel Property	Kernel Specification (EDF-6638, Rev. 0)		Measured Values (ORNL)	
	Average (95% conf)	Critical Limit (95% conf.)	Average (95% conf. range)	Critical Limit (95% conf.)
Mean Diameter (μm)	350 \pm 10	$\leq 1\%$ <300 and $\leq 1\%$ >400	357.0 – 357.6	<1% <332.3 and <1% >382.3
Aspect Ratio ($D_{\text{max}}/D_{\text{min}}$)	NA	$\leq 10\%$ ≥ 1.05	NA	<0.48% ≥ 1.05 <10% ≥ 1.026
Envelope Density (Mg/m^3)	≥ 10.4	NA	11.03-11.16	NA

Table 1-2. Summary of BWXT reported values¹ of LEU03 versus kernel specification.

Kernel Property	Kernel Specification (EDF-6638, Rev. 0)		Measured Values (BWXT)	
	Average (95% conf)	Critical Limit (95% conf.)	Average (95% conf. range or lower limit)	Critical Limit (95% conf.)
Mean Diameter (μm)	350 \pm 10	$\leq 1\%$ <300 and $\leq 1\%$ >400	356.9-360.4	<1% <333.1 and <1% >384.2
Aspect Ratio	NA	$\leq 10\%$ ≥ 1.05	NA	<4.7% $\geq 1.05^*$
Envelope Density (Mg/m^3)	≥ 10.4	NA	10.84-10.89	NA

* ORNL calculated from BWXT data

The BWXT results for measuring the same kernel properties are given in Table 1-2. BWXT characterization methods were significantly different from ORNL methods, which resulted in slight differences in the reported results. BWXT performed manual microscopy measurements for mean diameter (100 particles measured along 2 axes) and aspect ratio (100 particles measured); ORNL used automated image acquisition and analysis (3847 particles measured along 180 axes). Diameter measurements were in good agreement. The narrower confidence interval in the ORNL results for average mean diameter is due to the greater number of particles

measured. The critical limits for mean diameter reported at ORNL and BWXT are similar, because ORNL measured a larger standard deviation (10.46 μm vs. 8.70 μm).

Aspect ratio satisfied the specification with greater margin in the ORNL results mostly because of the larger sample size resulting in a lower uncertainty in the binomial distribution statistical calculation. ORNL measured 11 out of 3847 kernels exceeding the control limit (1.05); BWXT measured 1 out of 100 particles exceeding the control limit. BWXT used the aspect ratio of perpendicular diameters in a random image plane, where one diameter was a maximum or a minimum. ORNL used the aspect ratio of the absolute maximum and minimum diameters in a random image plane. The ORNL technique can be expected to yield higher measured aspect ratios. Hand tabling was performed at ORNL prior to characterization by repeatedly pouring a small fraction of the kernels in a pan and tilting the pan so that rounder kernels could roll down and drop through a slot in the pan, separating them from less round kernels, fragments and debris. A total of 0.37 g was removed in this manner from the 510 g composite. This can be expected to only produce a slight improvement in the ORNL aspect ratio acceptance value. The estimated change in the 95% confidence critical limit due to hand tabling, which was equivalent to removing 2-3 high aspect ratio kernels from the 3847 kernels in the measured sample, would be an increase from <0.48% to approximately <0.57% of the kernels in the composite predicted to have an aspect ratio greater than 1.05.

ORNL results for envelope density were about 0.2 Mg/m^3 higher than the BWXT results. This has always been the case when envelope density measurements have been compared between the two laboratories. As discussed in a previous report,² this is likely due to the Hg pressure used to define the envelope volume as well as differences in the measurement technique.

2 Size and shape measurement (Kercher, Hunn, Price)

2.1 Description of method

Size and shape were measured by shadow imaging a sample of LEU03 kernels in a random plane with an optical microscope. Image analysis software was used to find the center of each kernel and identify up to 360 points around the perimeter. The particle boundary was defined using a Fast Fourier Transform (FFT) fit (10 harmonics) for all regions that had points identified (i.e., no extrapolation). Data was extracted as both radius and diameter. The terms “radius” and “diameter” are used loosely. “Radius” means the distance from the Kasa fit center^{3,4} to the FFT boundary edge. “Diameter” means the distance from FFT boundary edge to FFT boundary edge on a line passing through the fit center. Data for each kernel was then reported in terms of the mean radius or diameter, the standard deviation in those values, the minimum and maximum radius and diameter, and the ratio of the maximum over the minimum of those values (aspect ratio). The uncertainty in the mean diameter for a single kernel was about $\pm 0.2 \mu\text{m}$. The error in the diameter aspect ratio of a single kernel was calculated to be less than 0.001. These values for each kernel were then compiled and the average, standard deviation, minimum, and maximum for each value was calculated. In addition to reporting the compiled data for the sample, histograms of the mean kernel radius or diameter and the aspect ratios have also been provided to show how these values were distributed in the analyzed sample.

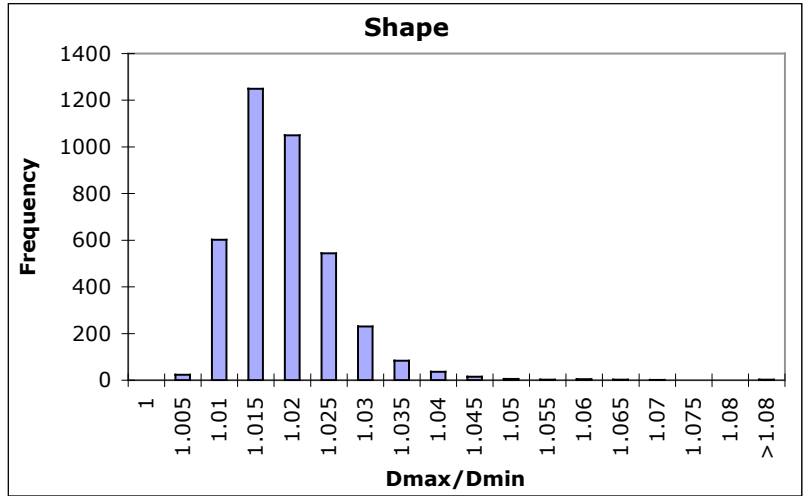
2.2 Size and aspect ratios

Fig. 2-1 shows the summary data for the measured diameter of 3847 kernel shadowgraphs. Fig. 2-2 shows the same data reported in terms of the radius. The difference between compiling the measurements in terms of radius versus diameter is that the radius based measurements more accurately report non-symmetric shapes. The diameter measurements dilute the effect of a local deviation in radius by adding the opposite radius (+180 degrees in polar coordinates). The average mean diameter was $357.3 \mu\text{m}$. The mean and standard deviation for radius was one half of the values reported for diameter. However, the radius aspect ratio and diameter aspect ratio (max/min) were quite different, because these values were based on maximum and minimums as opposed to means. Radius aspect ratio, $R_{\text{max}}/R_{\text{min}}$, is a more sensitive way of measuring the deviation from perfectly spherical. The radius aspect ratio measurement showed a higher average and standard deviation (avg. 1.027; $\sigma=0.013$) than the diameter aspect ratio (avg. 1.016; $\sigma=0.007$).

	Diameter Aspect Ratio	Mean Diameter	St. Dev. In Diameter	Minimum Diameter	Maximum Diameter
Average	1.016	357.3	1.6	354.4	360.2
Standard Deviation	0.007	10.5	0.7	10.4	10.7
Minimum	1.004	319.2	0.3	294.0	330.9
Maximum	1.148	390.4	15.8	380.1	402.6

Histograms are top-binned.

Aspect Ratio (D)	Frequency
1	0
1.005	23
1.01	602
1.015	1249
1.02	1049
1.025	544
1.03	230
1.035	83
1.04	36
1.045	15
1.05	5
1.055	2
1.06	4
1.065	2
1.07	1
1.075	0
1.08	0
>1.08	2



Mean Diameter	Frequency
300	0
305	0
310	0
315	0
320	1
325	0
330	2
335	73
340	138
345	308
350	465
355	550
360	592
365	775
370	567
375	232
380	120
385	23
390	0
395	1
400	0
>400	0

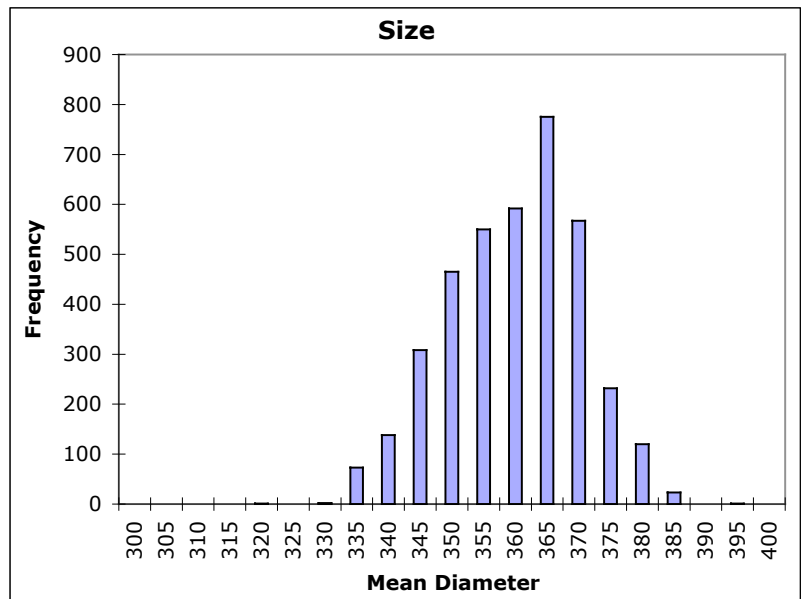
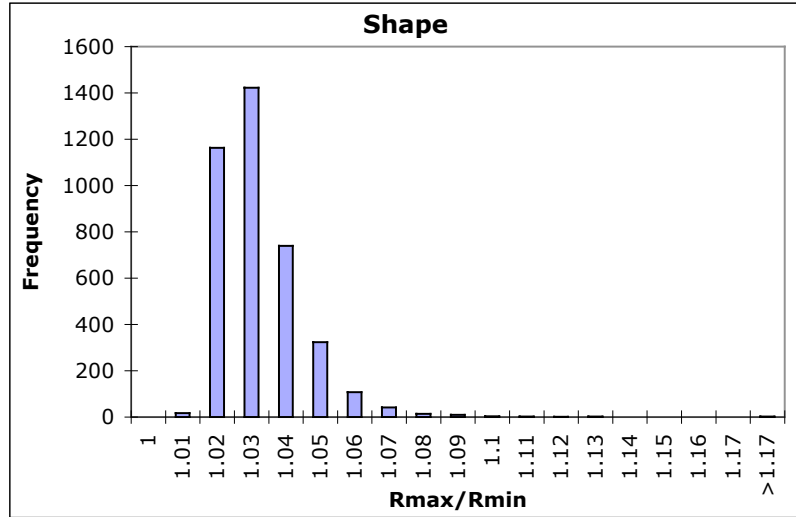


Fig. 2-1. Size and shape summary for 3847 LEU03 kernels. Diameter measurements are in μm from edge to edge through best circle fit center.

	Radius Aspect Ratio	Mean Radius	St. Dev. In Radius	Minimum Radius	Maximum Radius
Average	1.027	178.7	1.03	176.2	181.0
Standard Deviation	0.013	5.2	0.4	5.3	5.5
Minimum	1.006	160.6	0.2	144.2	166.4
Maximum	1.275	195.2	10.5	189.8	204.6

Histograms are top-binned.

Aspect Ratio (R)	Frequency
1	0
1.01	17
1.02	1163
1.03	1422
1.04	739
1.05	323
1.06	107
1.07	42
1.08	14
1.09	10
1.1	3
1.11	2
1.12	1
1.13	2
1.14	0
1.15	0
1.16	0
1.17	0
>1.17	2



Mean Radius	Frequency
150	0
152	0
154	0
156	0
158	0
160	0
162	1
164	0
166	15
168	85
170	113
172	250
174	337
176	390
178	455
180	484
182	591
184	574
186	296
188	143
190	90
192	22
194	0
196	1
198	0
200	0
More	0

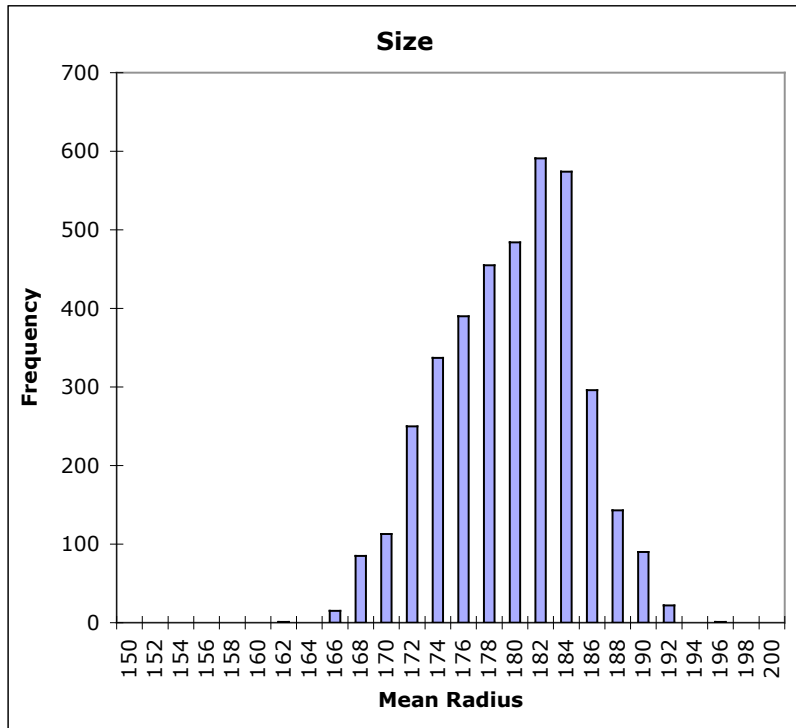


Fig. 2-2. Size and shape summary for 3847 LEU03 kernels. Radius measurements are distance from best circle fit center to edge in μm .

3 Optical and electron microscopy of kernel surfaces (Hunn, Menchhofer, Kercher)

As shown in Fig. 3-1, two different kernel types with different surface appearances can be readily identified in this composite lot of LEU03 kernels: shiny and smooth kernels (Type A) and dull and smooth kernels (Type B). Type A and B kernels are similar to those identified as Type 1 and 2, respectively, in a previous report on LEUCO (LEU01) kernels also fabricated by BWXT.² LEU03 kernels clearly do not have as wide of a microstructural variability as previously analyzed LEU01 kernels, which had four distinct kernel types.² Because a similar variety of kernel types was observed previously for a single batch of NUCO kernels,⁵ this microstructural variation is thought to be due to a non-uniformity in the forming or heat treatment processes rather than to batch to batch variability.

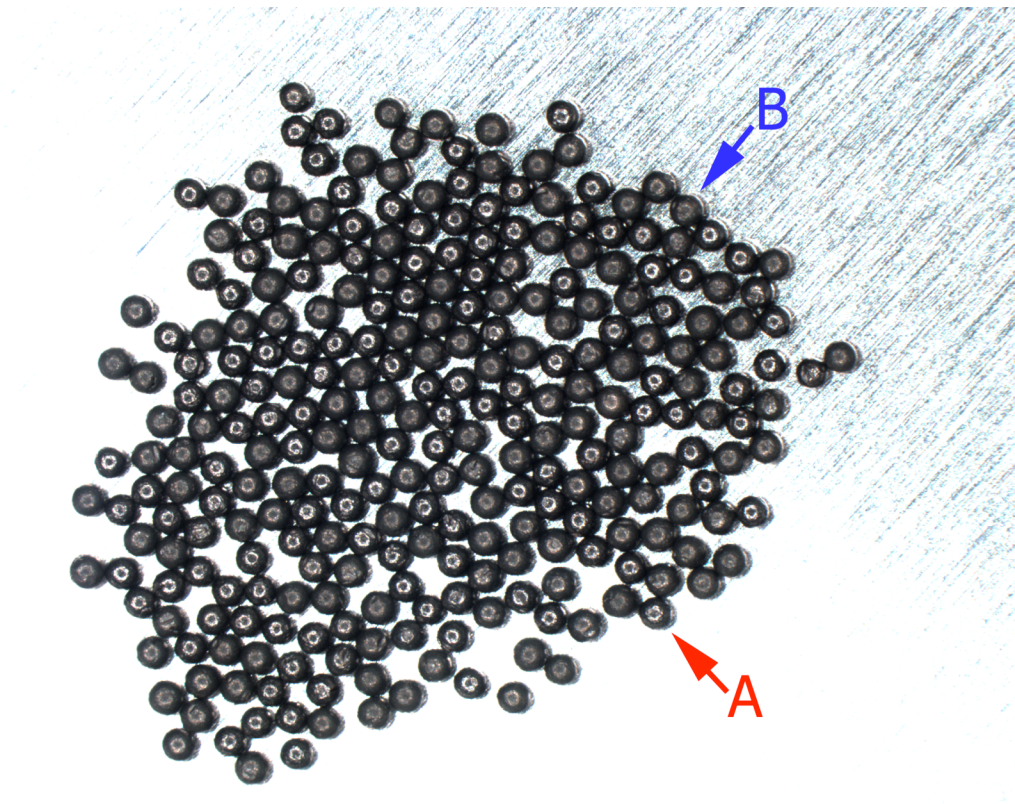


Fig. 3-1. This stereoscope image of a typical sample of LEU03 kernels shows a population of two kernel types: shiny and smooth (Type A) and dull and smooth (Type B). The circular ring observed on the Type A kernels (and faintly on Type B kernels) is a reflection of the ring light on the stereo microscope. Kernel diameter is approximately 350 μm .

3.1 Type A kernels (shiny & smooth)

Approximately 50% of the LEU03 composite lot was comprised of Type A kernels (shiny and smooth). Scanning electron microscope (SEM) images of a Type A kernel are shown in Fig. 3-2 and Fig. 3-3. The Type A kernel was fairly uniform in appearance with small, slightly recessed regions. This particular Type A kernel exhibited a large crevice (~60 μm long) which may be related to the large “wormholes” discussed in section 4.

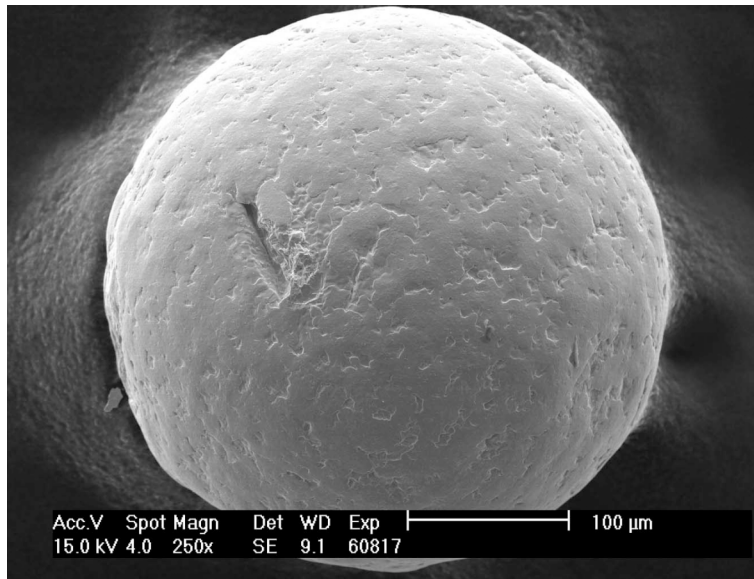


Fig. 3-2. Low magnification secondary electron image of a Type A kernel.

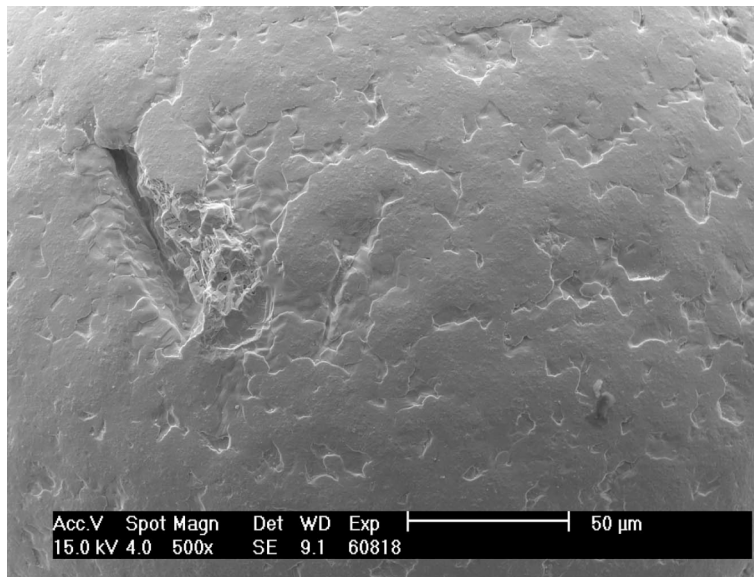


Fig. 3-3. Secondary electron image of Type A kernel showing average surface and large crevice.

3.2 Type B kernels (dull & smooth)

Approximately 50% of the LEU03 composite lot was comprised of Type B kernels (dull and smooth). Type B kernels were very similar to Type A kernels, but the overall surface was bumpier, making it less optically reflective. SEM images of a Type B kernel are shown in Fig. 3-4 and Fig. 3-5. This particular Type B kernel showed a large depression (see the center of the image in Fig. 3-4). These depressions were observed on at least half of kernels analyzed and often showed a common characteristic of having one linear edge similar to that in the figures below.

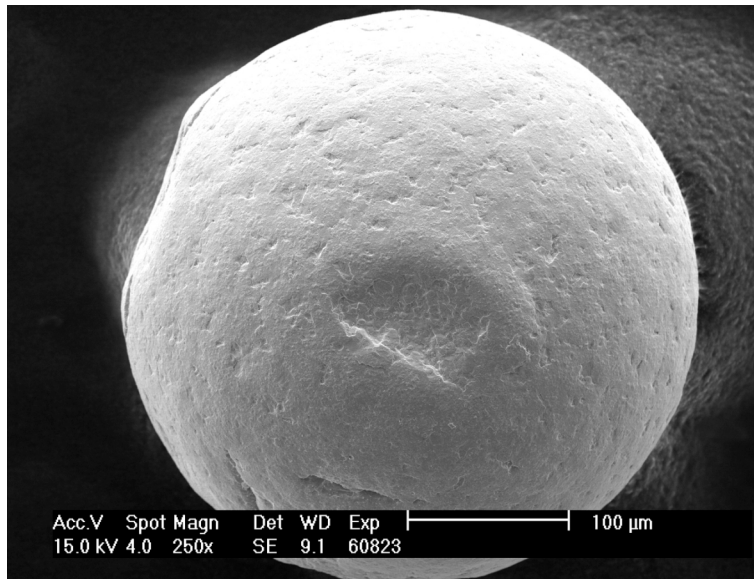


Fig. 3-4. Low magnification secondary electron image of a Type B kernel.

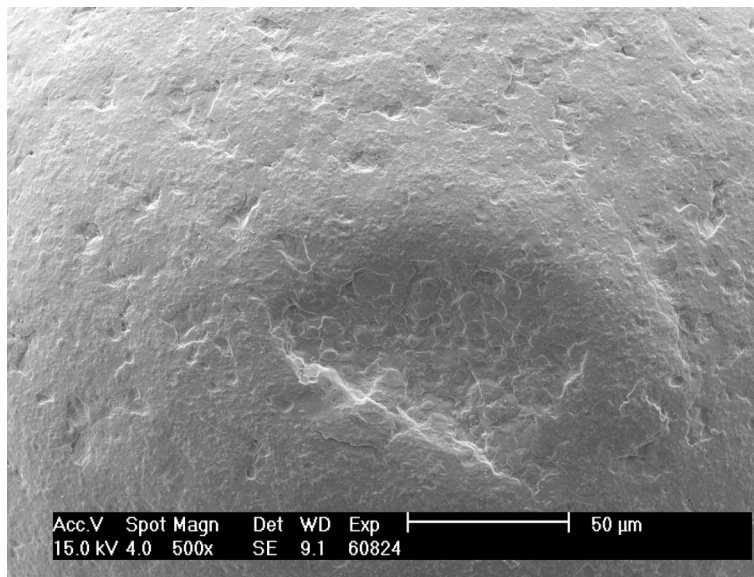


Fig. 3-5. Secondary electron image of a Type B kernel showing a large depression.

4 Microscopy of kernel polished cross-sections (Hunn, Menchhofer, Kercher, Dunbar)

LEU03 kernels were mounted in epoxy and ground and polished to near the midplane. A contrast variation across the cross section was readily observed both optically (Fig. 4-1 and Fig. 4-2) and by SEM using back-scattered electrons (Fig. 4-3). The darker gray areas were oxides and the lighter areas were carbides. A larger grain oxide rind was evident on the outside surface of all the kernels observed (Fig. 4-4 and Fig. 4-5b). The interior of the kernels showed a mixture of oxide and carbide regions (Fig. 4-4 and Fig. 4-5a).

The carbide regions contained both monocarbide (UC) and dicarbide ($UC_{1.86}$) phases. These two phases could be distinguished using back-scattered electron imaging (Fig. 4-6). This variation was due to the density difference and has been discussed in previous reports.^{2,5,6} Within each carbide region, the lighter areas are monocarbide and the medium gray areas (slightly lighter than the oxide regions) are dicarbide.

Pits (black spots) were observed in the LEU03 kernel cross sections (Fig. 4-5 and Fig. 4-6). These pits were observed to be predominantly in the oxide regions. Some pitting is caused by material removal during polishing but, based on their shape and location, most of the observed pitting was probably due to closed porosity in the kernels.

Some LEU03 kernels showed “worm holes” extending from the surface into the interior (Fig. 4-2 and Fig. 4-7). These features are likely related to surface crevices of the type shown in Fig. 3-2. It is not known if these crevices and worm holes are limited to type A kernels or if they appear in both types because the kernel type cannot be distinguished in the cross section images. Note that the oxide rind extends into the kernel to surround these worm holes, which indicates their presence during kernel fabrication as opposed to being an artifact of the sample preparation.

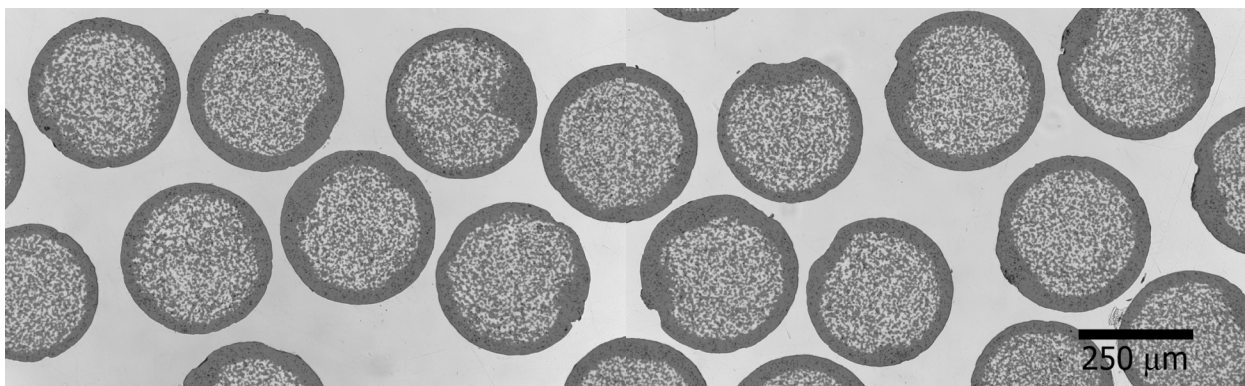


Fig. 4-1. Tiled optical micrographs of LEU03 cross-sections.

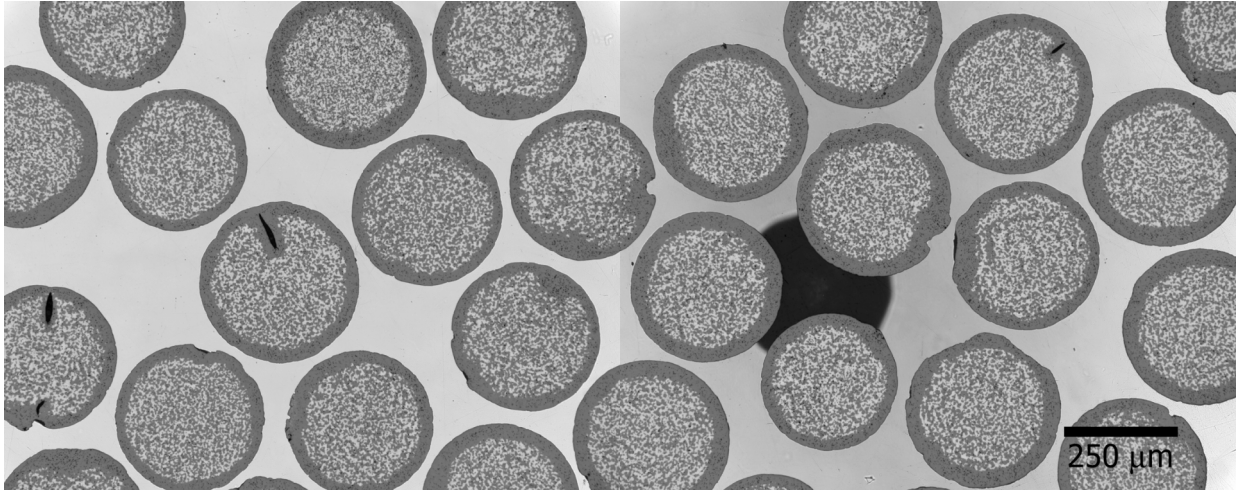


Fig. 4-2. Tiled optical micrographs of LEU03 cross-sections.

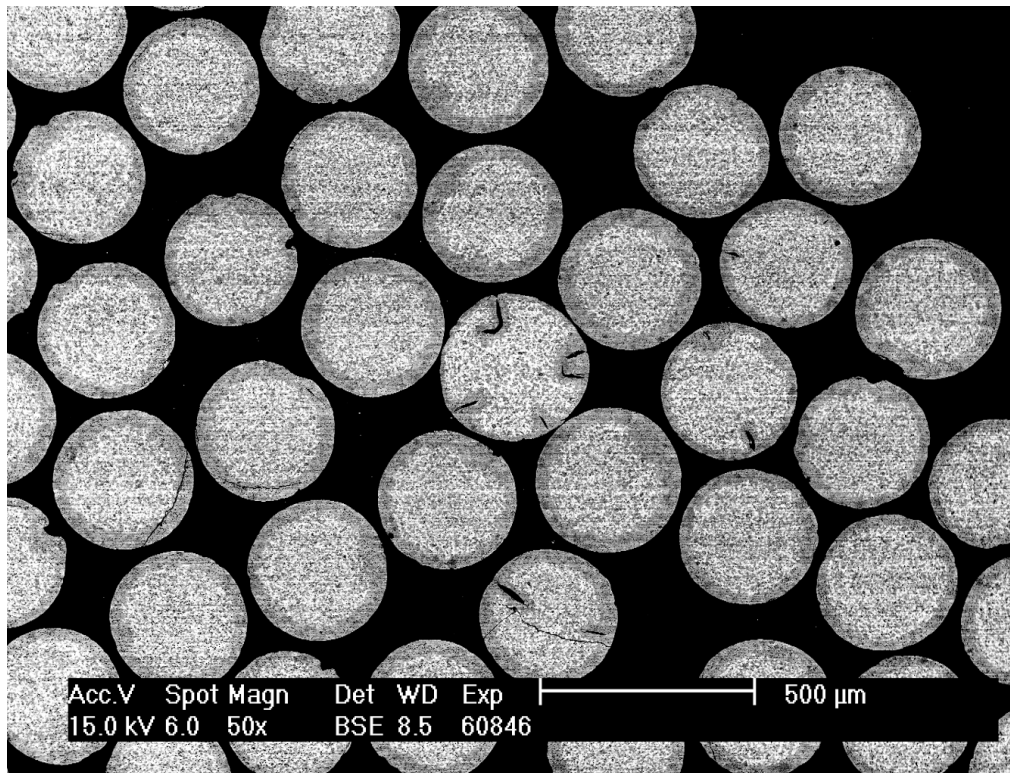


Fig. 4-3. Backscattered electron image of polished LEU03 cross-sections. Kernels exhibit an oxide ring and a two-phase core. Note the kernels with worm hole shaped open pores, which are likely related to the open crevices observed on the kernel surface.

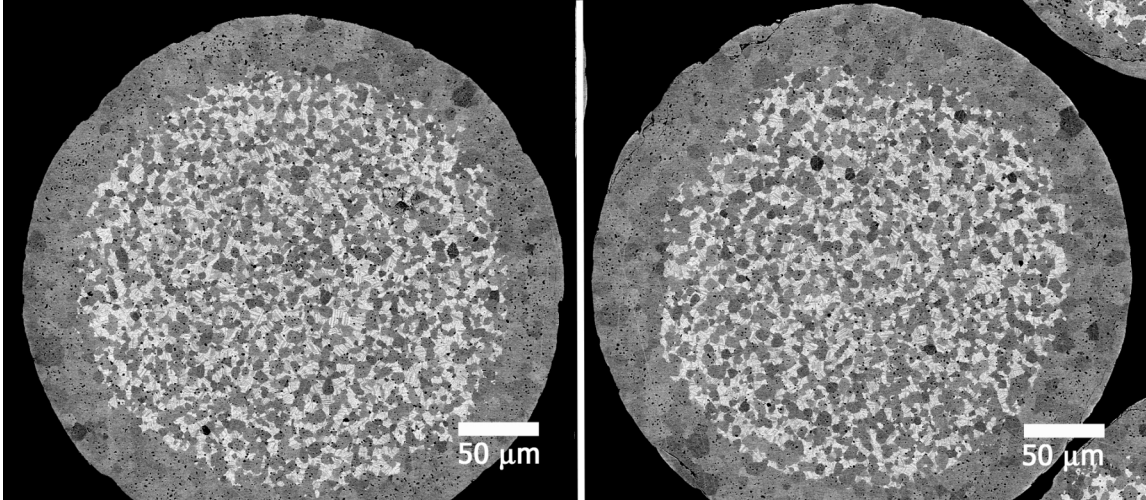


Fig. 4-4. Backscattered electron images of two polished LEU03 cross-sections.

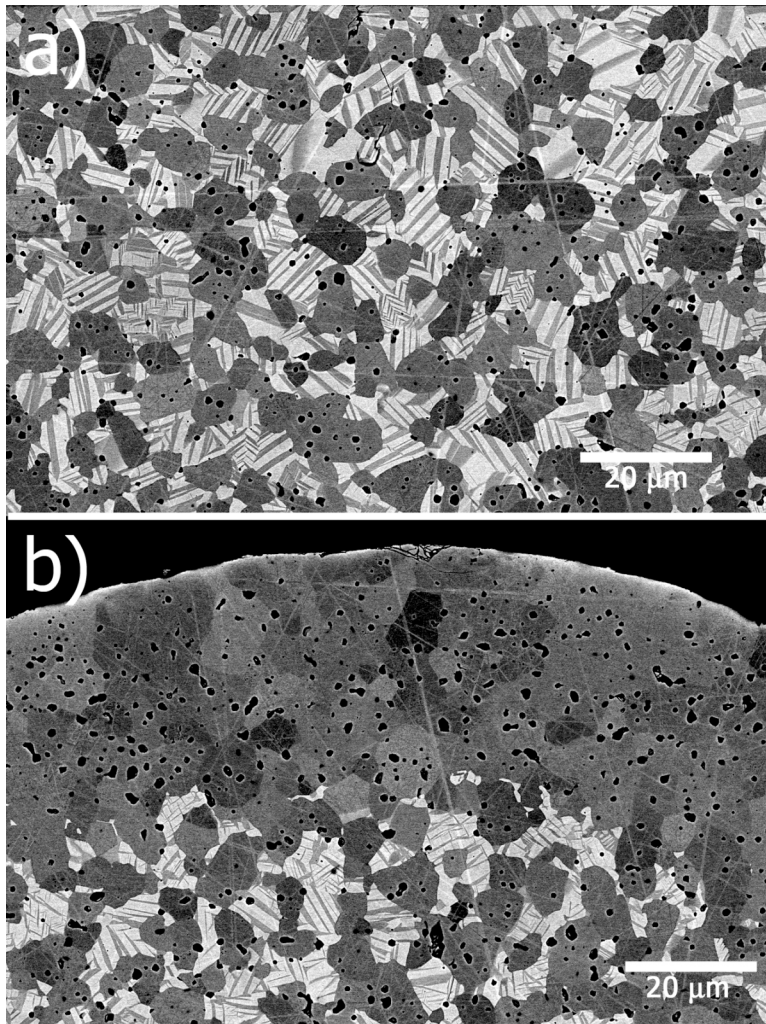


Fig. 4-5. Backscattered electron images of: (a) a central region of a kernel and (b) an outer region of a kernel.

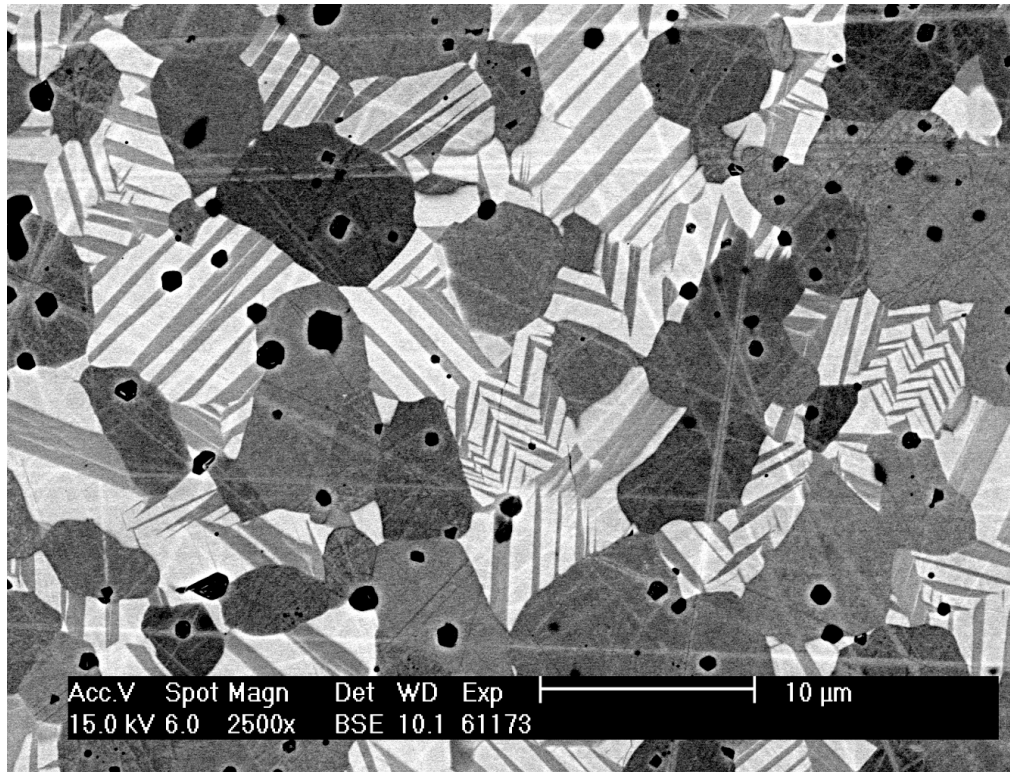


Fig. 4-6. Backscattered electron image of kernel showing oxide regions (solid gray grains) and carbide regions (lighter striated grains). The striations in the carbide regions are due to density variation between monocarbide (lighter areas) and dicarbide (medium gray areas).

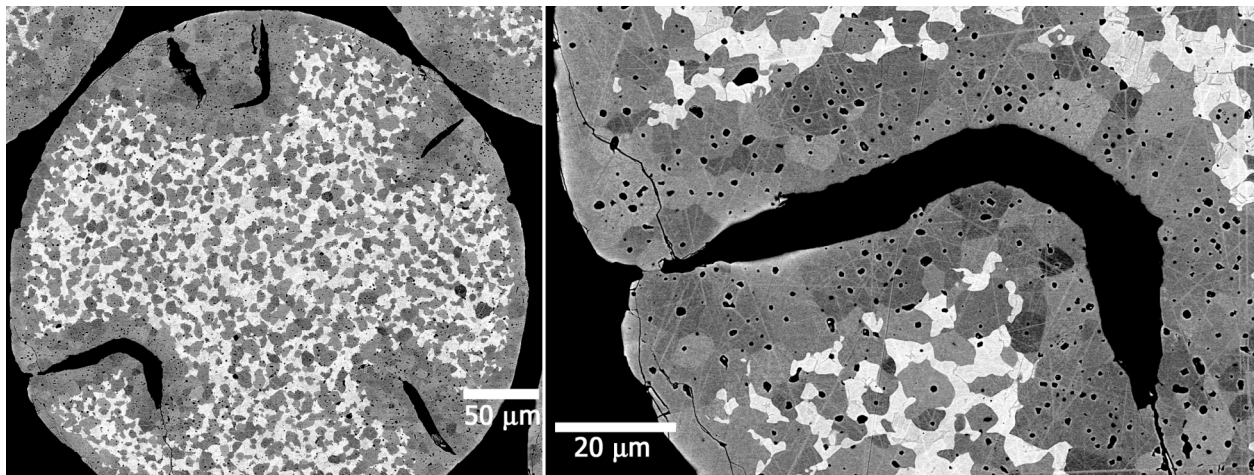


Fig. 4-7. Backscattered electron images of kernel with worm hole shaped open porosity. Note the carbon depleted zones surrounding the worm holes.

5 Density measurement (Hunn, Nunn)

Using the ASTM D3766 standard terminology, we define four different types of density: the *theoretical density* is based solely on the solid material volume, the *skeletal density* includes the closed pore volume, the *envelope density* includes the open and closed pore volume, and the *bulk density* includes the open and closed pore volume and the interparticle space. The theoretical density of UO_2 is 10.96 Mg/m^3 . The theoretical density of UC_2 is 11.28 Mg/m^3 . The theoretical density of UC is 13.63 Mg/m^3 . Envelope density was measured with a mercury porosimeter. The mercury pressure used to determine envelope density can have a significant effect on the reported value. The envelope density for this report was measured by weighing a sample and measuring the volume of mercury displaced at 25 psia. The Washburn equation for cylindrical pores, using an assumed Hg contact angle of 155° and surface tension of 480 dynes/cm, predicts mercury can fill pores of approximately $10 \mu\text{m}$ diameter at 25 psia. Thus, craters and large surface pores ($>10 \mu\text{m}$ diameter) were not included in the envelope volume.

The envelope density was measured on three samples riffled from the LEU03 composite. Table 5-1 shows the results. The average envelope density was 11.098 Mg/m^3 with a standard deviation of 0.025 Mg/m^3 .

Table 5-1. Envelope density by Hg porosimetry with 25 psia intrusion pressure

Sample weight (g)	Envelope density (Mg/m^3)
12.787	11.117
12.800	11.070
12.735	11.106

Average envelope density (Mg/m^3)	11.098
Standard Deviation (sample) (Mg/m^3)	0.025

References

¹ BWXT Nuclear Products Division, “G73 Industrial Fuel Fabrication and Development Lot G73V-20-69303”

² A.K. Kercher and J.D. Hunn, “Results from ORNL characterization of nominal 350 μm LEUCO kernels from the BWXT G73D-20-69302 composite,” ORNL/TM-2005/517.

³ I. Kasa, “A circle fitting procedure and its error analysis,” IEEE Transactions on Instrumentation and Measurement 25 (1976) 8-14.

⁴ C. Rusu, M. Tico, E. Kuosmanen, and E. Delp, “Classical geometrical approach to circle fitting – review and new developments,” Journal of Electronic Imaging; 12 (2003) 179-193.

⁵ J.D. Hunn, “Results from ORNL characterization of nominal 350 μm NUCO kernels from the BWXT 59344 batch.” ORNL/TM-2005/541.

⁶ J.D. Hunn, “Results from ORNL characterization of nominal 350 μm NUCO kernels from the BWXT 69300 composite.” ORNL/TM-2005/545.